ASNC IMAGING GUIDELINES FOR NUCLEAR CARDIOLOGY PROCEDURES

Equilibrium radionuclide angiocardiography

James R. Corbett, MD, Chair,[a] Olakunle O. Akinboboye, MD, BS, MPH, MBA,[b] Stephen L. Bacharach, PhD,[c] Jeffrey S. Borer, MD,[d] Elias H. Botvinick, MD,[e] E. Gordon DePuey, MD,[f] Edward P. Ficaro, PhD,[g] Christopher L. Hansen, MD,[h] Milena J. Henzlova, MD,[i] and Serge Van Kriekinge, PhD[j]

I. PLANAR IMAGING

A. Purpose

Planar equilibrium radionuclide angiocardiography (ERNA) is used to determine global and regional measures of ventricular function (primarily left ventricular [LV] function) at rest and/or during exercise stress or pharmacologic intervention. These measures of ventricular function may include evaluations of ventricular wall motion, ejection fraction (EF), and other parameters of systolic and diastolic function. The following sections provide a technical description of the techniques to acquire and process the data necessary to assess parameters of ventricular performance.

B. Radiopharmaceuticals

1. Inject the patient with technetium 99m-labeled red blood cells, with activity of approximately 20 to 25 mCi/70 kg body weight (11 to 13 MBq/kg) to provide the radioisotope tag for resting studies (Table 1). For exercise studies, the activity can be increased to 25 to 35 mCi/70 kg patient. The radiation dosimetry to the patient from 20 mCi of Tc-99m-labeled red blood cells labeled in vitro is 0.3 to 0.52 rem effective dose equivalent. With in vivo labeling of red blood cells, doses will run at the higher end of this range.[1]
2. Labeling methods.
   a. In vivo or modified in vivo/in vitro methods (e.g., using 2 to 3 mg stannous pyrophosphate 15 minutes before injection of the radiopharmaceutical).[2]
   b. Commercial in vitro kit.[3]

Quality control-labeling efficiency. Poor labeling of red blood cells can be easily recognized on ERNA images. Free Tc-99m-pertechnetate accumulates in the mucosa of the stomach and in the thyroid gland. A number of frequently used drugs and solutions are known to interfere with red blood cell labeling (Table 2).[4] Heparin unfavorably affects labeling efficiency. Thus, if at all possible, Tc-99m-pertechnetate should not be injected in heparinized intravenous lines, or they should be flushed thoroughly. Similarly, intravenous lines containing dextrose solution may alter labeling efficiency. In addition, antibodies against red blood cells may inhibit labeling. Antibodies may develop as a result of drugs such as methyldopa and penicillin. Antibodies may also be present in patients with chronic lymphocytic leukemia, non-Hodgkin's lymphoma, and systemic lupus erythematosus.

Labeling efficiency is also diminished when ''old'' Tc-99m-pertechnetate of low specific activity is used. Tc-99m decays to Tc-99, which is no longer useful for imaging but nevertheless competes with the radioactive form of stannous ions. To prevent the presence of carrier Tc-99, the Tc-99m dose should be taken from relatively fresh (<24 hours after elution) eluate from the generator.[5]

C. Acquisition Parameters—Rest/Exercise Imaging

1. *Collimator.* For resting studies, use of a parallel-hole, high-resolution collimator with spatial resolution of approximately 8 to 10 mm full width at half

Unless reaffirmed, retired, or amended by express action of the Board of Directors of the American Society of Nuclear Cardiology, this Imaging Guideline shall expire as of January 2014.

From the University of Michigan Health System,[a] Ann Arbor, MI; New York Hospital,[b] Flushing, NY; UCSF,[c] San Francisco, CA; New York Hospital-Cornell,[d] New York, NY; UCSF Department of Medicine,[e] San Francisco, CA; St. Lukeós-Roosevelt Hospital,[f] New York, NY; University of Michigan,[g] Ann Arbor, MI; Jefferson Heart Institute,[h] Philadelphia, PA; Mount Sinai Medical Center,[i] New York, NY and Cedars-Sinai Medical Center,[j] Los Angeles, CA.

Reprint requests: James R. Corbett, MD, Chair, University of Michigan Health System, Ann Arbor, MI.

1071-3581/$34.00

doi:10.1007/s12350-008-9027-z

Table 1. Radiopharmaceuticals used for planar ERNA

	Rest	Exercise		For information, see paragraph
Radiopharmaceutical	Tc-99m-labeled RBCs	Tc-99m-labeled RBCs	Standard	1
Dose	20–25 mCi/70 kg	25–35 mCi/70 kg	Preferred	1
Labeling method	In vivo	In vivo	Not recommended	2
	Modified in vivo/ in vitro	Modified in vivo/ in vitro	Standard	2
	In vitro	In vitro	Preferred	2

Table 2. Causes of poor red blood cell labeling

Cause	Mechanism
Hydralazine	Oxidation of stannous ion
Prazosin	Decreases labeling rate
Propranolol	Increases dissociation
Digoxin	Decreases labeling rate
Doxorubicin	?
Iodinated contrast	?
Heparin	Complexes with Tc-99m Oxidation of stannous ion
Dextrose	Complexes with Tc-99m
Methyldopa	Induces RBC antibodies Oxidation of stannous ion
Penicillin	Induces RBC antibodies
Quinidine	Induces RBC antibodies
Immune disorders	Induces RBC antibodies
Prolonged generator ingrowth	Increased carrier
Decreased hematocrit	Relative increase in plasma which oxidizes stannous ion (?)
Excess stannous ion	Tc-99m reduced outside the RBC
Insufficient stannous ion	Incomplete reduction with free Tc-99m pertechnetate

RBC, Red blood cell
From Gerson MC. Cardiac nuclear medicine. 3rd ed. New York: McGraw-Hill; 1997. Reproduced with permission of the McGraw-Hill Companies

maximum (FWHM) (of a line spread function) or better at 10 cm distance from the collimator, as well as a sensitivity (for Tc) of approximately 4,000 to 5,000 counts $\cdot$ s^{-1} $\cdot$ mCi^{-1} (108 to 135 counts $\cdot$ s^{-1} $\cdot$ MBq^{-1}), is preferred (Table 3). If a time-limited stress study (e.g., bicycle exercise) is to be performed, a higher sensitivity (and therefore poorer spatial resolution) collimator may be considered, such as a low-energy all-purpose (LEAP) collimator (typically 12 mm FWHM at 10 cm and sensitivity of approximately 10,000 counts $\cdot$ s^{-1} $\cdot$ mCi^{-1}, or approximately 280 counts $\cdot$ s^{-1} $\cdot$ MBq^{-1}), or optionally a high-sensitivity collimator. In this case, it is especially important to keep the collimator–chest wall distance minimized. It is recommended that the same collimator be used for both the rest and stress study, with parallel-hole LEAP collimator being preferred. If caudal tilt is used (see paragraph 10), a slant-hole collimator may be considered instead of a parallel-hole collimator to provide 10° to 15° of caudal tilt while maintaining minimal collimator–chest wall distance.

2. *Pixel size*. Any matrix size that results in a pixel size less than approximately 4 mm/pixel (with approximately 2 to 3 mm/pixel being preferred) can be used. These acquisitions are usually performed using a zoomed 64 $\times$ 64 matrix of 16-bit (word) pixels. The zoom required to meet the less than 4 mm/pixel criteria will depend on the field of view (FOV) of the camera used. Minimal to no zoom is recommended for small-FOV cameras (circular, 10 inch diameter, or square, 8 inch) to zoom factors of 1.5 to 2.2 for large-FOV (rectangular, 21 inch) cameras. Smaller-FOV cameras, if available, are preferred. In any case, pixel size should not exceed 5 mm. See paragraph 5.
3. *FOV*. The effective FOV is dependent on the camera size and acquisition zoom utilized. Typically, an 18 $\times$ 18-cm^2 FOV will be sufficient, but any FOV size sufficient to encompass all four cardiac chambers and at least 2 cm beyond the cardiac blood pool (for positioning of a background region of interest [ROI]) is acceptable. Larger FOVs are acceptable, provided that they (1) do not inhibit minimizing collimator–chest distance and (2) are not so large as to cause increased gamma camera dead time. If large FOVs are used, care must be taken to prevent

Table 3. Camera/computer setup[6-11]

	Rest	Exercise		For information, see paragraph
Collimator	Parallel—LEAP	Parallel—LEAP	Preferred	1
(rest/exercise)	Parallel—high sensitivity	Parallel—high sensitivity	Optional	1
Collimator	Parallel—high resolution		Preferred	1
(rest only)	Parallel—LEAP		Optional	1
	Slant hole	Slant hole	Optional	1
Pixel size	<4 mm/pixel	<4 mm/pixel	Standard	2, 3
	2-3 mm/pixel	2-3 mm/pixel	Preferred	2, 3
Energy window	140 keV, ±10%	140 keV, ±10%	Standard	4
Bad beat	Buffered beat	Buffered beat	Preferred	5
	On-the-fly:	On-the-fly:	Standard	5
	Reject beat and next beat	Reject beat and next beat	Preferred	5
Beat length window	±10-15%	±10-15%	Standard	5
	Check trigger	Check trigger	Preferred	5
Acquisition method	Frame mode	Frame mode	Standard	7
	List mode	List mode	Optional	7
Frame rate (EF)	>16 frames/cycle	16-32 frames/cycle	Standard	8
	24-32 frames/cycle	24-32 frames/cycle	Preferred	8
Count density	>1800/pixel (3 mm) or 20,000/cm^2 (high-resolution collimator)	Not applicable	Standard	9
	>3600/pixel (3 mm) or 40,000/cm^2 (high-sensitivity collimator)	2-3 minutes acquisition	Standard	9
Positioning	LAO (best right/left separation)	LAO (best right/left separation)	Standard	10a
	LAO (caudal tilt)	LAO (caudal tilt)	Optional	10a
	Plus anterior, lateral		Standard	10b and 10c
Quality control	View cine loop	View cine loop	Preferred	6
	R-R histogram	R-R histogram	Preferred	6

acquisitions terminated on liver or spleen overflow and to ensure that data are displayed with cardiac structures at maximum intensity. Use of a lead apron as a shield for the liver/spleen may be appropriate, positioned with the aid of a persistence scope.

4. *Energy window.* 140 keV, ±10% window.
5. *Bad beat/beat length window (arrhythmia rejection).*[8,12,13] If systolic function only (EF) is to be assessed, accepting less than 10% to 15% arrhythmic beats are acceptable. If the examination is performed to determine diastolic function, beat length windowing (arrhythmia rejection) is necessary. The preferred arrhythmia rejection mode is buffered beat, where each beat is temporarily stored in memory to assess whether its beat length is within the (typical) ±10% to 15% R-R beat length window. If the beat is outside the window, it is rejected without contaminating the gated data acquired. Standard arrhythmia rejection methods typically terminate data acquisition if a premature beat is seen outside of the (±10% to 15%) beat length window (a portion of the bad beat will be acquired). Rejection of the short or long beat along with rejection of the subsequent (compensatory) beat is preferred. The typical beat length window is ±10% to 15% but will vary depending on heart rate and rhythm. If the study is acquired with significant arrhythmias, poor statistics may result, and accurate computation of EF may be compromised. The beat length window may require lengthening to improve statistics but will compromise measurement of diastolic function and may adversely affect cine-loop displays if end frames are not corrected or deleted. See paragraph 8. With regard to triggers, assessment of the adequacy of the R-wave trigger prior to instigation of the gated acquisition should be performed. It is recommended that the electrocardiographic (ECG) trigger point be checked to ensure that the ECG gating circuitry is synchronized to the peak of the ECG R-wave. Checks can be either performed visually, with a dual-trace oscilloscope, or checked with a commercially available dynamic phantom. Poor-quality or delayed triggers can adversely affect the ventricular volume curve.
6. *Post-acquisition quality control of the ERNA study is also recommended.* Visualization of the beating cine loop after acquisition allows evaluation of data drop-off due to inadequate triggers, significant arrhythmias, rhythm disorders, poor tag, or poor count statistics. Review of the beat-length R–R interval histogram can be used to assess cardiac rhythm abnormalities or determine if significant arrhythmias were present. Quality control can anticipate errors associated with inadequate ERNA studies prior to the reporting of ventricular performance.
7. *Acquisition method.* Frame mode gating is standard (forward framing), although forward/backward, as well as forward/backward by thirds, methods are optional. If arrhythmias are present, the frames at the end of the cardiac cycle (containing data acquired over shorter total acquisition time) should be either corrected or deleted (preferred). List-mode data acquisition is optional and offers increased beat length windowing flexibility, particularly for analysis of diastolic function.[6]
8. *Frame rate.*[12] A frame rate of less than 50 milliseconds/frame is preferred for resting EF. A frame rate of less than 30 milliseconds/frame is preferred if ejection and filling rates are to be computed. For rest studies, a minimum of 16 to 19 frames per cardiac cycle is recommended, with 24 or 32 being preferred for EF calculation and for calculation of ejection and filling parameters. For stress studies (R–R <600 milliseconds), 32 frames/cycle is preferred for EF calculation and calculation of peak ejection and filling rates.
9. *Count density.* Studies containing approximately 20,000 counts/cm^2 (1,800 counts/pixel for a 3-mm pixel) over the center of the left ventricle at rest using high-resolution collimation, or about 40,000 counts/cm^2 at rest with the higher-sensitivity collimators (LEAP or high sensitivity), as used in rest/exercise studies, are preferred (which corresponds to about 3 to 4 million counts in a 15 × 15-cm^2 FOV with high-resolution collimator). This count density is measured by summing all images in the gated series together and determining the count density from a small ROI at the center of the left ventricle in the left anterior oblique (LAO) projection. Total counts are not a reliable indicator, as they depend too strongly on the FOV. Nevertheless, a practical rule has been to acquire at least 200,000 counts per image frame for a 16-frame resting study using a high-resolution collimator. Similarly, acquisition time will give variable results depending on collimator sensitivity. To calculate a typical acquisition time, for a particular collimator and dose, sum all frames in the study together, and using a small ROI at the center of the left ventricle, determine the time necessary to achieve the above-mentioned counts per square centimeter. During stress, acquisition time is often the limiting factor. When this is the case, at least 2 minutes (preferably 3 minutes) of acquisition time at peak stress is recommended using the LEAP or high-sensitivity collimator, as previously specified.

10. *Camera positioning—imaging angles.* To acquire the ERNA study, position the patient supine (for greatest patient comfort) or in the right lateral decubitus position (to minimize interference from diaphragm and spleen). Three views should be recorded for assessment of wall motion of the left ventricle.

    a. *LAO view.* The LAO view is optimized to visualize the septum (best septal view—usually the 45° LAO, but the angle will depend on body habitus and cardiac orientation) (Figure 1). In the LAO view, the orientation should be such that the long axis of the ventricle is approximately vertical, with the apex pointing down and left ventricle on the right side of the image. Caudal tilt of the LAO view, typically 10° to 15°, is helpful to separate the atria from the ventricle and may be particularly useful in patients with vertical hearts. The degree of caudal tilt is limited by the detector yoke suspension and the necessity to keep the camera face as close as possible to the chest. As an alternative to achieve a 10° to 15° caudal tilt, a slant-hole collimator may be used, if available. When using a caudal tilt, depending on the imaging conditions, the LV and left atrial separation still may not be apparent. This may result in inclusion of more left atrium than desired, if the atrial-ventricular border is difficult to discern, as the superior aspect of the ROI may encroach into the left atrium. If the atrial-ventricular border is not evident, use the standard LAO view. On a correctly angulated LAO projection, the photopenic area of the septum is more or less vertical. To the left is the foreshortened right ventricle. The right atrium is partially hidden behind and superior to the right ventricle. At the viewer's right, the LV blood pool is well isolated from the surrounding structures by the myocardium as a photopenic halo. The appendage of the left atrium can occasionally be seen superior to the left ventricle, usually separated from the LV blood pool by the photopenic area of myocardium. As a rule, LV blood pool is projected as nearly a ''short-axis'' view. In other

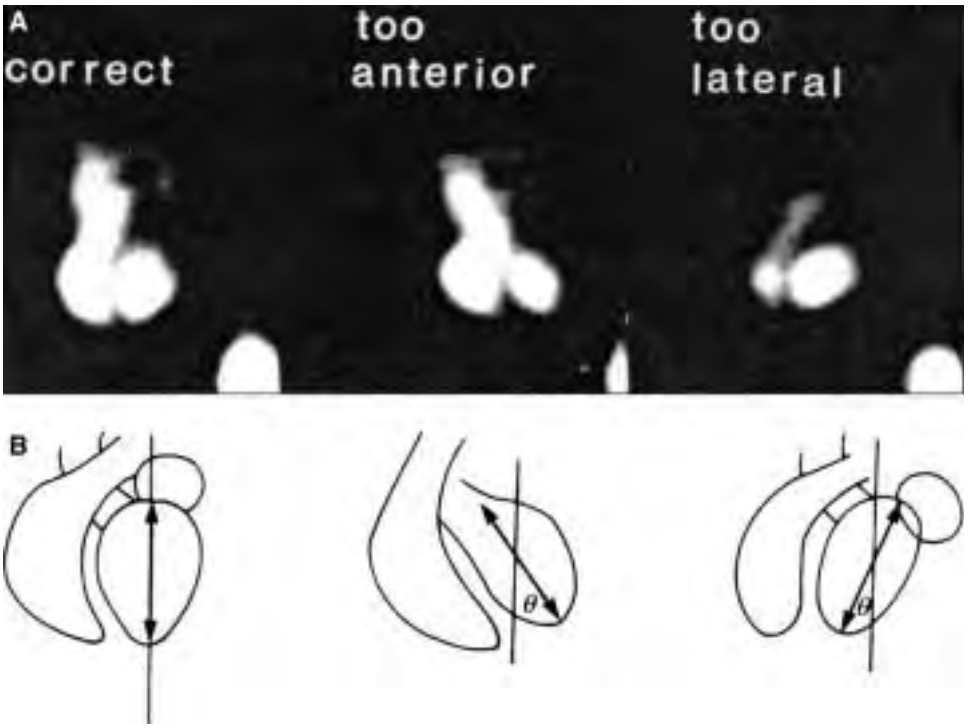

Figure 1. Correct positioning to image left ventricle.[8] **A**, LAO images that are optimal, too anterior, and too lateral in obliquity. **B,** In an optimized LAO view the axis of the left ventricle should be vertical. In images that are too anterior, there is a rightward tilting of the axis from base to apex. In images that are too laterally positioned, there is a leftward tilting of the axis from base to apex. (Reproduced with permission from DePuey.[8]).

words, one looks ''down the barrel'' of the left ventricle. In some patients, the heart is vertically oriented. This anatomic variant can be recognized because of the elongated shape of both ventricles and visualization of both the right atrium and left atrium superior to the ventricles. The pulmonary artery and ascending aorta can also be evaluated in the LAO view. The myocardial segments typically visualized in the LAO view are the septal, inferoseptal, inferoapical, inferolateral, and lateral. The two other preferred views are as follows:

b. *Anterior view*. The anterior view ideally should be −45° more anterior than the LAO selected. On the anterior view, the border-forming contour on the right side of the heart (left side of image) is the right atrium. To the viewer's right, the border-forming contour of the heart on this view is the left ventricle. Because of the overlying activity of the right ventricle, only the anterolateral wall and apex can be evaluated. The inferior wall is frequently completely obscured by the right ventricular (RV) blood pool. Further structures that can be evaluated on the anterior view are the pulmonary artery and the ascending aorta. The myocardial segments typically visualized in the anterior view are the basal anterolateral, mid anterolateral, apical, mid inferoseptal, and basal inferoseptal.
c. *Lateral view*. The left lateral or left posterior oblique (LPO) view; the LPO view angle selected is +45° more lateral than the LAO view angle selected. These views are best acquired with the patient lying on his or her right side. An optimal left lateral view shows the long axis of the left ventricle. ''Long axis'' is defined as the longest dimension from valve plane to apex. Because there is individual variation among patients, either the straight left lateral or the LPO view may show the long axis of the left ventricle best. In the left lateral projection, the left ventricle is superimposed on activity of the right ventricle. Anterior and superior to the left ventricle, the RV outflow tract and the pulmonary artery can be noted. The mitral valve plane is often well demarcated by a linear photopenic area caused by attenuation by fatty tissue in the atrioventricular groove. Posterior to the left ventricle are the left atrium and the descending aorta. The spleen is usually visualized in the right lower corner of the image. The myocardial segments typically visualized in the lateral or LPO view are the basal anterior, mid anterior, apical, mid inferior, and basal inferior.

D. Assessments of Ventricular Function—ERNA at Rest: Image Display and Quantification (Table 4)

1. *Display.*[6,8,10,11] Multiple-view ERNA (LAO, anterior, and left lateral or posterior oblique projections) are usually displayed simultaneously as endless-loop movies in quadrants of the computer screen. The display should visualize the entire heart and its surroundings. ERNA images are best viewed by use of a linear gray scale. Color display is strongly discouraged. Occasionally, intense extracardiac activity may cause a problem with image display. Computer images are usually normalized to the hottest pixel within the image over all time points. In the presence of intense extracardiac activity, radioactivity in the heart is at the darker (lower) end of the gray scale and may be almost invisible. Rather than using lead shielding, normalization of the cardiac image to the hottest pixel within the heart usually deals adequately with this display problem. Alternatively, the extracardiac activity may be subtracted or ''masked out''.
2. *Smoothing*.[15,16] The smoothing process is designed to remove statistical fluctuations from image data by modifying individual data points within the image. Multiframe digitized ERNA data are often temporally and spatially smoothed. For temporal smoothing, pixels are modified by weighted averaging of data from preceding and following frames in time, usually 3 to 5, with the center pixel replaced with this average value. For spatial smoothing, pixels are modified by weighted averaging of counts from a group of neighboring pixels within the same image, usually 9, with the center pixel in the group replaced with this weighted average value. This is referred to as Gaussian 9-point weighted smoothing. The exact number of temporal or spatial points used for the smoothing will depend on the number of time points acquired and the acquisition resolution. Images of adequate count density rarely require spatial smoothing.
3. *LV volume curve generation.*[17-20] Most parameters describing ventricular function are extracted from a complete LV volume curve or time-activity curve (TAC). This curve can be obtained either from a single ROI drawn at end diastole (and modified at end systole, if necessary, to include any dyskinetic regions) or preferably using multiple ROIs drawn at each time point. ROIs should be edited on an amplitude or difference image to exclude overlapping atrial counts. Manually drawn ROIs are the most consistently accurate, though time consuming. Many

Table 4. Quantitative parameters of ventricular function–planar ERNA[6,8,10,11,14]

Parameter	Method		For information, see paragraph
LV volume curve generation	Manual ROI at ED and ES	Preferred	3
	Manual or automatic ROIs at each time point	Optional	3
	Manual or automatic ROIs at ED only	Optional	3
Background	Manual at ED	Preferred	4
	Automatic at ED	Standard	4
	Automatic or manual at ES	Optional	4
LVEF	From end-diastolic and end-systolic ROIs	Preferred	5
	From Fourier-filtered curve	Optional	5
	From single end-diastolic ROI (not recommended)	Optional	5
LV wall motion	Visual assessment of cine loop	Preferred	6a
	Phase and amplitude analysis	Optional	6b
	Principal component or factor analysis	Optional	6c
	Regional EF	Optional	6d
LV emptying	Peak rate of emptying	Preferred	7a
	Average rate of emptying	Optional	7b
	Time to peak emptying rate	Optional	7a
LV filling	Peak rate of filling	Preferred	8
	Average rate of filling	Optional	8
	Time to peak filling rate	Optional	8
LV volumes	Counts based	Optional	9
	Geometric based	Optional	9
RVEF	Not widely accepted at equilibrium	Optional	10
Heart/lung ratio	Counts based LV/lung	Optional	13

automatic techniques exist for drawing ROIs. It is important that the resulting ROIs be checked visually and altered manually if necessary. Irregularities in LV contours occasionally occur using automatic algorithms, especially for exercise studies, and for ROIs drawn near end systole. These irregularities can have significant effects on parameters extracted from the LV curve. If EF only is to be determined, the preferred method (and the simplest) for LV volume curve generation is from manually drawn ROIs over end diastole and end systole, with the volume curve being processed by weighted interpolation of curves from end-diastolic and end-systolic ROIs (weighted to end diastole near the beginning and end of the curve and weighted to end systole at curve minimum). If ejection and filling rates are to be computed, ROIs drawn on all frames are preferred. **NOTE:** Single ROI definition at end diastole may underestimate EF. Optionally, automatic edge detection may be used, if each frame is reviewed, and the ROI corrected, if necessary.

4. *Background*. Background is critical for the measurement of many LV parameters. Usually an ROI 5 to 10 mm away from the end-diastolic border, drawn from approximately 2 o'clock to 5 o'clock, is used, although the exact location used is less important than consistent placement, ensuring that atrial counts, counts from the spleen or descending thoracic aorta, LV counts, or a gastric air bubble is excluded. With automatic routines, visual verification of the background ROI is essential. A visual examination of the TAC produced from the background ROI (it should be flat) is useful to determine if LV activity or atrial activity is spilling into the background ROI. If the background curve is flat, this indicates that the background ROI has not been positioned over any periodically beating structures and that all time points may be averaged for good statistics. An ROI adjacent to the end-systolic border can be used to estimate background, but care must be taken to use only those time points that do not include LV activity. A rule of thumb is that the background count rate/pixel is

typically 30% to 70% of the end-diastolic LV counts, and exceptions to this rule occur infrequently.

5. *LVEF*.[6-8,13,14] Many methods are commercially available for computation of LVEF. In general, LVEF is calculated based on the assumption that LV volumes throughout the cardiac cycle are proportional to LV counts. LV counts at end diastole and at end systole or throughout the cardiac cycle are measured by constructing LV ROIs. The measured LV counts within these LV ROIs are corrected for background scatter. Background is measured using ROIs constructed adjacent to the lateral or inferoapical walls of the ventricle. LV ROI counts are corrected for background by subtracting background counts from LV ROI counts. This is referred to as background correction (BkCorr). LVEF then is calculated using the usual equation: ([End-diastolic volume (EDV) − End-systolic volume (ESV)]/EDV) × 100 or, as applied to ERNA, LVEF = ([BkCorr end-diastolic counts − BkCorr end-systolic counts]/BkCorr end-diastolic counts) × 100.

   Three basic approaches are commonly employed.

   a. LVEF can be computed by selecting only the end-diastolic and end-systolic frames and constructing the appropriate LV and background ROIs. This is just as effective as using all frames from the entire cardiac cycle, and if regions are being constructed manually, this greatly decreases processing time. No matter what the approach, care must be taken to ensure that LV ROIs are appropriately fitted to include all LV counts, but only LV counts (i.e., LV ROIs) should not extend to include the activity from any adjacent structures such as the left atrium above, right ventricle to the left, an adjacent intensely active spleen below and to the right, or a grossly ectatic descending aorta immediately to the right. Automatically generated LV ROIs may need to be edited or redrawn by the operator if they do not tightly fit the apparent LV boundaries. This is especially the case at end systole, where automatically generated ROIs often do not fit well, extending irregularly beyond the ventricle frequently including the aortic root to the left and beyond the apex above. If the end-systolic LV ROI is not correctly drawn, the calculated LVEF will generally be underestimated.
   b. If all frames throughout the cardiac cycle are employed to generate an LV TAC, one optional method that can be used fits two or four Fourier harmonics to the LV TAC, extracting the first and the minimum points, as the end-diastolic and end-systolic count values. Because this method uses the entire curve, it reduces statistical fluctuations, even for very short (stress) acquisitions. If the first point of the filtered curve is used, one must ensure that the ECG gate is correctly set up, with gating occurring no later than the peak of the R wave, preferably during the upslope of the R wave to ensure that the first point truly corresponds to end diastole. If the R-wave trigger is not precisely at end diastole (see section I.C.5, ''Bad beat/beat length window [arrhythmia rejection]''), then the maximum value of the filtered curve can be used to identify the end-diastolic counts. Fourier fitting may fail to provide reliable results if there is ''drop off'' in TAC counts at the end of the curve due to heart rate variability from sinus arrhythmia or other arrhythmias varying the R–R′ interval. This effectively reduces the time of acquisition of frames at the end of the diastolic phase of the cardiac cycle and the corresponding TAC. Fourier filtering should be applied only to curves that have no drop off or that have been corrected for drop off.
   c. EF can also be computed from the LV counts produced from a single end-diastolic ROI, applied to both the end-diastolic and the end-systolic images. In this case, the EF will be consistently underestimated compared to the above methods. The single end-diastolic LV ROI approach is discouraged.

6. *LV wall motion*.[15,16,21-27]

   a. Visual assessment of all three standard views is preferred. It is critical that the cine loop consist of approximately 12 to 16 frames (fewer frames may lose temporal information, greater may compromise statistics). If the acquisition is performed with more than 16 frames for improved temporal resolution, it is imperative that the frames be appropriately added/recombined or filtered before visual assessment. Spatial filtering and temporal filtering are often employed in cine-loop presentations. Spatial filtering is typically a 9-point spatial smooth and reduces the apparent quantum mottle or image noise. Temporal filtering typically weights the current frame two parts and the previous and postframes one part to recreate the cine-loop image with 16 frames or more. Both types of filtering tend to make the cine loop appear more visually pleasing. If rest and stress are to be compared, it is preferred to show both cine loops simultaneously. Optionally, modern application of principal components analysis (PCA) or factor analysis can create a mathematically derived cine loop which separates various types of wall motion

(atrial, ventricular), producing a more visually pleasing motion image, reducing the appearance of noise in the cine. However, the effects of PCA analysis on the assessment of regional wall motion have not been completely evaluated.

b. Phase and amplitude images have been reported to be of use for the detection and quantification of wall motion defects. It is preferred that this method supplement, not replace, visual assessment of the cine loop. Analyses of the phase image and phase histogram, as well as visual assessment of a dynamic phase image, have both been reported to be useful in reducing the subjectivity associated with visual assessment of wall motion defects using cine loops. Also, in patients with conduction abnormalities, phase analysis has proven useful in identifying the pattern, location, and/or point of origin of arrhythmic foci.

c. PCA or factor analysis creates a mathematically derived set of functional images expressing significant motion components in the image. Displayed as amplitude images and associated time signatures, they may add to the assessment of regional wall motion and can be viewed in similar fashion to phase and amplitude images or applied to process the cine-loop display (see above). This method is clearly a supplement at this point and should be used in conjunction with standard cine-loop assessment of wall motion. (d) Regional EF (i.e., dividing the left ventricle into 6 to 8 subregions and applying the conventional formulation for EF) has been reported to aid in the assessment of regional or segmental wall motion. It is preferred that this method supplement, not replace, visual assessment of the cine loop.

Cardiac rhythm and conduction.[8,13,28,29] Because the ERNA is formatted and displayed as an endless-loop cine of a single representative beat, the ''rhythm'' always looks regular. Abnormalities of rhythm can only be discerned by the relationship of atrial to ventricular contraction. The most common sustained disturbance of rhythm is atrial fibrillation. Atrial fibrillation or flutter can be assumed to be present when no atrial contraction is detected. Occasionally, one may diagnose flutter or atrial tachycardia by a difference between the atrial and ventricular contraction rates—that is, 2 or 3 atrial contractions to each ventricular contraction. A pacemaker rhythm is usually apparent because the LV activation starts at the apex, and the wave front of contractions proceeds to the base. Left bundle branch block can be diagnosed by the typical paradoxical pattern of septal motion.

7. *LV emptying*.[12,30]

   a. The maximal LV emptying rate is determined by measuring the peak slope of the LV curve, expressed in units of EDV/second. The counts in the end-diastolic ROI are used to represent the EDV, and the counts in subsequent frames are referenced to this value to compute EDV/second. The time to peak emptying (from the end-diastolic frame) may also be computed and expressed in milliseconds. Measurement error in the down slope of the LV volume curve is greatly amplified by statistical noise in the unprocessed (unfiltered) curve. For this reason, either the LV curve is generally first filtered or a small region of the curve is fitted to a polynomial, or other similar techniques are employed to minimize noise without distorting the value of slope. Measurements of peak emptying at exercise are often considered too heart rate dependent or statistically inadequate to be of clinical use. When computing peak or maximal emptying rate, 32 frames per cardiac cycle is preferred to ensure accurate assessment of maximal rate.

   b. The slope of a line connecting the end-diastolic and end-systolic points can be used as a measure of the average LV emptying rate. Alternatively, methods that depend on the time it takes for the left ventricle to empty one-third (or any other arbitrary fraction) of the way from end diastole to end systole have been reported.

8. *LV filling/diastolic function*.[8,12,31-35] The same techniques described in paragraph 7 above can be used to measure diastolic filling rates. All of the same considerations mentioned above for emptying also hold for filling. Note that the gating requirements for adequate representation of diastolic parameters are more stringent than for systolic ejection parameters, due to data drop off at the end of the cardiac cycle.

   Qualitative. Visual analysis of the shape of the LV TAC is frequently sufficient to detect gross abnormalities of diastolic filling. Prolongation of isovolumic relaxation, a delay in the onset of rapid filling, a decrease in the slope of the rapid filling phase, or an exaggerated contribution of atrial contraction to LV filling may be readily apparent and should be noted. Such findings are typical of hypertrophic ventricles. Aging, pericardial disease, and restrictive myocardial disease are also

associated with changes in the pattern of filling and a decrease in the rate of filling.

Quantitative. Peak diastolic filling rate can be quantified from the first derivative of the diastolic portion of the LV TAC. To obtain reliable values for diastolic filling, the LV volume curve should have sufficient temporal resolution. Values for normal studies vary from laboratory to laboratory, but a generally accepted lower limit of normal for the peak diastolic filling rate (PFR) is 2.50 EDV/second. PFR tends to decrease with age in otherwise healthy older subjects. In addition to the PFR, the time to PFR (tPFR) can also be measured from the LV TAC and is expressed in milliseconds. As with the PFR, the tPFR also varies from laboratory to laboratory but on average should be expected to be less than 180 milliseconds. The relative contribution of atrial filling to LV filling may be quantified as the ratio of the atrial peak to the peak of the rapid filling phase on the first derivative curve. Ratios of less than 1:4 are normal but may increase with aging.

9. *LV volumes*.[36-40] Acceptable results have been reported in the literature using both counts-based and (to a lesser extent) geometrically based methods, although counts-based methods are preferred. Geometric methods are based on the standard ''area-length'' methods and are hampered by the limited spatial resolution of ERNA. Both the counts-based and geometrically based methods may produce highly inaccurate results unless extraordinary attention is paid to methodological detail. These methods are not widely used. Assessments of LV volume are affected by photon attenuation and Compton scatter. Counts-based methods include the ''aortic arch'' method or methods involving blood draws and calibration of the counts-to-volume ratio. The latter method is highly influenced by photon attenuation. Calculation of absolute volumes is not recommended, except for laboratories that have the ability to independently validate their methodology.
10. *RVEF*.[41-44] Because of overlap with other cardiac chambers, ERNA is not the procedure of choice for measurement of RVEF. Frequently, there is overlap of right atrial activity during RV systole, which will lead to an erroneously low calculation of RVEF. Overlap of the right atrial activity with the right ventricle may be partially circumvented by acquiring a separate shallower LAO, about 20° LAO, chosen to optimize the separation of the right ventricle from both the right atrium and left ventricle. Although optimal separation is generally impossible, improved separation usually is relatively easily accomplished. Rotating slant-hole collimators, if available, may be quite useful in optimizing atrioventricular separation. Either true first-pass or ''gated first-pass'' radionuclide angiocardiography is the preferred approach. Both of those techniques yield RVEF values that are higher than those measured on a standard ERNA study. The lower limit of normal with these methods is 0.40.
11. *RV size*. This is best evaluated in the anterior view. Assuming that ERNA images are routinely acquired with the same gamma camera and same zoom factor, abnormal enlargement of the right ventricle can be identified by visual inspection and mental comparison to normal studies. There is no reliable quantitative measurement method for the RV volume with ERNA.
12. *RV regional wall motion*. This is best assessed by use of the information from both the anterior and LAO views. Any single view may be inadequate. Regional wall motion is usually qualitatively graded as normal, mildly hypokinetic, severely hypokinetic, akinetic, or dyskinetic.
13. *Heart/lung ratio.* Optionally, heart/lung ratio can be computed. The ratio of the counts in the cardiac blood pool to the counts in the lung can be useful to assess ventricular compensation. Pooling of blood in the lungs has been reported to be indicative of LV failure.

E. Assessment of Ventricular Function During Exercise and Interventions: Image Display and Quantification[7,8,11,45,46]

1. *Display*. ERNA images acquired at baseline and during exercise or pharmacologic interventions should be displayed side by side on quadrants of the computer screen for evaluation of changes between the two sets of images.
2. *Regional wall motion changes from rest*.[45,47-49] One should expect an increase in regional excursion during exercise, during inotropic stimulation, and during administration of afterload-reducing agents such as nitroglycerin. The standard approach to detection of changes in regional wall motion between two studies is to visually assess the change on the side-by-side display. A somewhat more rigorous approach is the semiquantitative method in which ventricular segments are assigned scores where 4 is normal, 3 is mildly hypokinetic, 2 is moderately

hypokinetic, 1 is severely hypokinetic, 0 is akinetic, and −1 is dyskinetic. A significant change in regional wall motion between two studies is defined as a change in score of 2 or greater.

3. *Chamber size changes from rest*.[50-52] During interventions, changes in chamber size may occur. A mild increase in end-diastolic volume is normal during physical exercise, especially with patients in the upright position.[50] During dobutamine stress, a decrease in LV chamber size may be observed. These changes may be too small to be appreciated by visual analysis but can be quantified either as a relative change (from decay-corrected count changes) or absolute volume change. Visually, only moderate to severe dilation of the ventricles should be reported. Such marked volume changes are almost always abnormal. If volume is measured quantitatively, one should expect increases in LV EDV of only 10% to 20% during exercise and concomitant decreases in ESV.
4. *LVEF and RVEF changes from rest*.[12,43,47,48,53-57] Both LVEF and RVEF typically increase during exercise. Many authors have suggested that the normal response is an increase of at least 5%, or 5 EF units. That criterion is based on the reproducibility of the ERNA measurements of LVEF. Nevertheless, this criterion does not hold true under all circumstances. For instance, with increasing age, the ability to augment LVEF during exercise decreases. The type of exercise protocol, the subject's gender, acquisition during submaximal exercise, isometric exercise, markedly hypertensive responses to exercise, and coexisting noncoronary heart disease may all alter the response of the EF to exercise. Consequently, a failure to increase LVEF of at least 5% is a sensitive but very nonspecific criterion for diagnosis of coronary heart disease. In the absence of an exercise-induced regional wall motion abnormality, changes in LVEF alone are nonspecific. Coupled with a large (>20%) increase in EDV during exercise, a drop in LVEF with normal regional wall motion during exercise should be viewed as highly suspicious for coronary artery disease.

   A more important parameter is the absolute level of LVEF at peak exercise. Even if angiographic coronary artery disease is documented, a peak exercise LVEF greater than 50% indicates a favorable prognosis. It is important to ensure that acquisition of radionuclide data is performed during peak exercise. In most patients, with and without significant disease, a significant increase in LVEF can be noted immediately after discontinuation of exercise. Abnormalities in RVEF during exercise are most often seen in patients with chronic pulmonary diseases and in particular in those with pulmonary hypertension. Patients with cardiomyopathy and bi-ventricular dysfunction or proximal right coronary artery stenoses may also demonstrate abnormal RV responses.
5. *Comparison to previous studies and correlation with clinical data*.[45,55,58] When a patient has undergone previous radionuclide studies, the results of this study should be compared with the previous ones. Ideally, one should display the old and new studies side by side. Serial LVEF data are particularly important in patients undergoing chemotherapy for cancer and also in patients with heart failure, myocarditis, or cardiomyopathy or after undergoing transplantation. For this reason, it is helpful to record and reproduce the camera angles at which the three planar cardiac views are acquired for each study. Interpretation of ERNA data may be performed without knowledge of the clinical data; however, once an initial interpretation is made, the interpreting physician should always review the available clinical information to avoid obvious misinterpretation and to guarantee that the interpretation appropriately addresses the clinical question that prompted the study.
6. *Study quality*. Poor-quality studies cannot be interpreted with confidence and a high degree of reproducibility. Studies can be subjectively graded as (a) excellent, (b) average, (c) suboptimal but interpretable, and (d) uninterpretable. Placing such a designation in the report communicates a level of confidence in the data that is helpful to recipients of the report. It may also be used to screen studies from inclusion in research data. If possible poor-quality (suboptimal and uninterpretable) studies should be repeated but, if for some reason, they cannot be, the subjective grade of study quality will at least alert the referring clinician to the limited reliability of the reported results.
7. *Type of exercise or intervention protocol*.[50,59] The type of exercise should be specified in the report: physical exercise on treadmill or supine or upright bicycle. The exercise protocol should be stated. Exercise ERNA studies are performed with bicycle ergometers, and the levels of stress during each image acquisition are reported in watts or kilogrammeters of work and duration. Treadmill protocols such as the Bruce, modified Bruce, and Naughton protocol are not used with exercise ERNA. For pharmacologic intervention, the generic name of the

drug (e.g., dobutamine) and maximal dose (e.g., 40 mg · kg^{-1} · min^{-1}) infused should be stated. Furthermore, whether drugs were administered to either enhance or counteract the effect of the pharmacologic stressor should be reported.

8. *Symptoms, heart rate and blood pressure response, ECG changes, and endpoint of stress.* Within the report of the radionuclide study, a succinct description should be given of important clinical parameters: duration of exercise or stress protocol, baseline and peak stress heart rate, maximal workload (in metabolic equivalents when applicable), baseline and peak stress blood pressure, symptoms during test, (re)production of symptoms and chest pain, and ECG changes compared with baseline.

F. Image Analysis/Interpretation[7,8,10,11,39]

1. *Overall cardiac assessment.* The initial assessment of ERNA studies should include an overall general assessment of the size, position, and rotation of the cardiac blood pool (heart) and proximal great arteries. In most patients there is not a great deal of variability in regard to position and rotation if the standard best septal LAO, anterior, and lateral projections have been acquired. In patients with severe obstructive airways disease and patients with congenital heart disease, often previously undiagnosed, to mention only a few causes of significant variability, size, position, and rotation can differ greatly from the expected. The best septal projection can on rare occasion be as shallow as straight anterior or as steep as 10° to 30° LPO. If the technologist has not carefully identified and noted the angulation of the best septal LAO projection and the standard ''anterior'' (−45°) and ''lateral'' (+45°) projections, the quantification of ventricular function will be significantly impaired and the interpretation of segmental function of the left and right ventricles hampered by either chamber overlap or misidentification of segments or both. For example, if the interpreting physician does not note that the rotation of the heart in the sagittal oblique plane is quite steep in a patient with severe chronic obstructive pulmonary disease and depressed diaphragm, that individual may interpret motion at the base of the left ventricle in the LAO projection as anterior wall motion, as is more commonly the case in patients without overinflated lungs, rather than motion of the mitral valve plane. In patients with pulmonary hypertension, the right ventricle is often greatly dilated and, with this, the septum is often rotated to a steep LAO, lateral, or LPO projection. If the technologist does not recognize and note this during image acquisition, chamber overlap may be so severe that the left ventricle cannot be assessed at all.
2. *Attenuation artifacts*. As is the case for myocardial perfusion imaging, breast attenuation may also affect ERNA imaging. On the LAO view, the entire heart may be in the ''shadow'' of the left breast. At times, this may give the illusion of a halo around the heart and suggest pericardial fluid. Lack of ''swinging'' of the heart and the typical configuration of the shadow may provide clues for the artifact.
3. *Activity outside the heart and great vessels*. Any vascular structure (tumor, etc.) with a sufficient volume of red blood cells can be visualized by ERNA imaging. Therefore, it is important to be attentive for any unusual radioactivity outside the heart and great vessels and seek clinical correlation. Free Tc-99m-pertechnetate accumulates in the thyroid gland and gastric mucosa.
4. *Chamber sizes.*
   a. *LV size*. One can qualitatively assess the relative size of various cardiac chambers. This assumes that the same camera and magnification are used routinely. Because in many patients the right ventricle is normal in size and function, RV end-diastolic size may serve as a benchmark for qualitative assessment of the relative size of other cardiac structures. On a normal study, the right ventricle is usually somewhat larger than the left ventricle and the RV inferior wall and apex extends below the left ventricle. A normally sized left ventricle ''fits'' within the crescent of the right ventricle on the LAO view. The presence or absence of marked LV hypertrophy (LVH) can be estimated by qualitative assessment of the thickness of the septum. The septum is well delineated by RV and LV blood pool, and thus the thickness of the myocardium can be assessed. In severe LVH, a thick photopenic halo typically surrounds the LV blood pool.
   b. *RV size*. This is best evaluated in the anterior view. Assuming that ERNA images are routinely acquired with the same gamma camera and same zoom factor, abnormal enlargement of the right ventricle can be identified by visual inspection and mental comparison to normal studies. There is no reliable quantitative measurement method for the RV volume with ERNA.
   c. *Atrial sizes*. The right atrium forms the left lower border on the anterior view of the cardiac image. Size and contraction of the right atrium can be evaluated in this view during ventricular systole.

The left atrium is best evaluated on the left lateral view during ventricular systole. Because of overlying and surrounding radioactivity, frequently no clear outline of the left atrium is present. However, the general size and contractility of the left atrium usually can be appreciated. The size of the left atrium should be judged in comparison to the long axis of the left ventricle. The contraction of the left atrium is appreciated as a change in count density during ventricular diastole and is sometimes discernible on radionuclide studies.

Atrial contraction does, however, occur at the very end of the acquisition cycle. Atrial contraction is shorter than the ventricular cycle. In the presence of ventricular ectopy or irregular rhythm, the last frames have lower count density, resulting in ''flicker'' of the endless-loop cine. During processing, one or two frames at the end of the cycle may be ''cut off''' for aesthetic reasons. As a result, atrial contraction may no longer be evaluable.

5. *LVH*. The presence of LVH is best assessed in the LAO view as more than normal thickening of the septum. This is a subjective evaluation that requires familiarity with the normal appearance of the septum on ERNA images acquired with a particular gamma camera. In severe LVH, the LV blood pool is surrounded by a thick photopenic area—that is, the hypertrophied myocardium. During systole, there can be almost complete LV cavity obliteration.
6. *Pericardial space*. Pericardial fluid accumulation can be identified on ERNA studies. When a large amount of fluid is present, a photopenic area surrounds the heart, extending up to the roots of the large vessels. On the cine display, a swinging motion of the heart can be appreciated. When estimating the extent of the photopenic area around the ventricular blood pool, one should account for both the thickness of the myocardium and the presence of epicardial fat before deciding that pericardial fluid is present. Consequently, small amounts of fluid are impossible to distinguish from normal variants. The shadow of a large overlying breast may, particularly in the LAO view, mimic pericardial fluid. Only swinging motion of the heart is a certain sign of a large amount of pericardial fluid. The preferred technique to assess pericardial fluid continues to be echocardiography.
7. *Size of pulmonary artery and aorta*. The pulmonary artery and the ascending and descending aorta can also be evaluated visually on good-quality ERNA studies. Only qualitative assessments, such as dilation of the pulmonary artery and dilation and tortuosity of the ascending aorta, aortic arch, or descending aorta, can be made. The three conventional views allow for visual assessment from different angles.
8. *Conclusion*. It is important to summarize the results of the test as either ''normal'' or ''abnormal.'' Equivocal statements should be avoided if at all possible. In addition, the report should reflect the degree to which the test is abnormal: ''markedly,'' ''moderately,'' or ''mildly'' abnormal. Finally, a comparison should be made to previous results, if applicable. A serious attempt should be made to provide an answer to the clinical questions and indication for study.

II. SINGLE-PHOTON EMISSION COMPUTED TOMOGRAPHY IMAGING

A. Purpose

Single-photon emission computed tomography (SPECT) ERNA is used to determine global and regional measures of ventricular function (primarily LV function) at rest and/or during pharmacologic intervention. These measures of ventricular function may include evaluations of ventricular wall motion, EF, and other parameters of systolic and diastolic function. The following sections provide a technical description of the techniques to acquire and process the data necessary to assess parameters of ventricular performance.

B. Radiopharmaceuticals (Table 5)

1. Inject the patient with Tc-99m-labeled red blood cells, with activity of approximately 25 to 30 mCi/70 kg body weight (14–17 MBq/kg) to provide the radioisotope tag. With in vivo labeling or red blood cells, doses will run at the higher end of this range.[1]
2. Labeling methods.
   a. In vivo or modified in vivo/in vitro methods (e.g., using 2 to 3 mg stannous pyrophosphate 15 minutes before injection of the radiopharmaceutical).[2]
   b. Commercial in vitro kit.[3]

C. Acquisition Parameters and Reconstructions—Gated SPECT ERNA (Table 6)

1. *Camera*. Use of dual-detector (two-head) SPECT cameras in the 90° configuration are the most common preferred camera setup (90° gantry rotation required), but three-head cameras in 120° configurations are another preferred approach (120° rotation). For 360° image acquisitions, three-head SPECT systems (120° configuration) are the most efficient systems for image acquisition (120°

Table 5. Radiopharmaceuticals used for SPECT ERNA

			For information, see paragraph
Radiopharmaceutical	Tc-99m-labeled RBCs	Standard	1
Dose	25-35 mCi/70 kg	Preferred	1
Labeling method	In vivo	Not recommended	2
	Modified in vivo/in vitro	Standard	2
	In vitro	Preferred	2

RBC, Red blood cells

Table 6. Camera and computer setup and reconstruction[7,60-64]

	Data/method		For information, see paragraph
Camera and computer setup			
Camera	Dual-head—90° configuration	Preferred	1
	Three-head—120° configuration	Optional	1
	Single head	Optional	1
Collimator	Parallel—high resolution (dual head)	Preferred	2
	Parallel—LEAP (single head)	Preferred	2
Pixel size	4.8-6.6 mm/pixel	Standard	3
Energy window	140 keV, ±15%	Standard	4
Beat length window	±15-35%	Standard	5
Bad beat rejection	Reject beat	Standard	5
	Reject beat and next beat	Preferred	5
Acquisition method	Frame mode	Standard	6
Frame rate	16 frames/cycle over full cycle	Standard	7
	16 frames/cycle over partial cycle	Optional	7
Number of views	60-64	Standard	8
	30-32	Optional	8
	30-32 (single head)	Standard	8
Time per view (seconds)	20-30	Standard	8
	40-60	Optional	8
	40-60 (single head)	Standard	8
Acquisition stop mode	Time per view	Standard	8
	Cardiac cycles per view	Preferred	8
	Acquisition time per view	Preferred	8
Rotation	180°	Standard	9
	360°	Optional	9
Gated SPECT reconstruction parameters			
SPECT reconstruction	Filtered backprojection or iterative	Standard	10
Reconstruction filter	Butterworth 0.55 Nyquist cutoff		
	Order = 7	Standard	10
	Butterworth 0.45 Nyquist cutoff	Optional	10
Oblique reorientation	Short-axis oblique	Standard	11
	Long-axis coronal	Optional	11
	Long-axis sagittal	Optional	11

rotation acquisitions) followed by dual-head SPECT systems in a 180° configuration (180° rotation acquisitions). Single-head SPECT cameras are the least efficient systems for both 180° and 360° acquisitions, requiring 180° and 360° rotations, respectively, to acquire a full study. With multidetector SPECT systems, ERNA SPECT can be performed in half the time, about 15 minutes, of a 3-view planar ERNA series and are highly recommended. Dual-headed cameras in the 180° configuration are optional but are not recommended unless 360° image acquisitions are desired (180° rotations are required). Single-head SPECT cameras with 180° rotations are optional, but not recommended. Acquisition time with a single-head camera (180° rotation) is approximately 30 minutes.

2. *Collimator.* High-resolution parallel-hole collimators (resolution of approximately 8 to 10 mm FWHM or better at 10 cm and sensitivity [Tc] of approximately 4,000 to 5,000 counts $\cdot$ s^{-1} $\cdot$ mCi^{-1} [108 to 135 counts $\cdot$ s^{-1} $\cdot$ MBq^{-1}]) are preferred when using multidetector SPECT systems. LEAP collimators (typically 12 mm FWHM at 10 cm and sensitivity of approximately 10,000 counts $\cdot$ s^{-1} $\cdot$ mCi^{-1}, or approximately 280 counts $\cdot$ s^{-1} $\cdot$ MBq^{-1}) may be preferred when using a single-head SPECT camera.
3. *Pixel size*. A 64 $\times$ 64 matrix size of 16-bit word pixels or a 128 $\times$ 128 matrix size of 8-bit byte pixels is preferred. Acquisition zooms that result in pixels 4.8 to 6.6 mm^2 in the acquired planar projection images and comparably sized cubic voxels in the reconstructed SPECT image sets are standard of practice. Acquisitions may be performed using acquisition zooms as high as 1.75 with large-FOV cameras (1.75 for patients with small body habitus) providing pixels as small as 4 mm^2. However, it is critical that the entire cardiac blood pool be in the FOV in all projections or severe truncation artifacts may result. If pixel sizes smaller than 4.8 mm are desired, a test rotation with observation of the blood pool using a persistence scope in all views is recommended. With large-FOV rectangular detectors, common on most modern and currently available SPECT systems, a test orbit is only required in patients with very severely dilated hearts. Most quantification programs are validated at only one or two pixel/voxel sizes, and it is generally recommended that an acquisition zoom (voxel size) be used on all patients in keeping with the image input requirements of the quantification software used.
4. *Energy window*. 140 keV, ±15% window.
5. *Bad beat/beat length window (arrhythmia rejection)*. The preferred arrhythmia rejection mode is on-the-fly bad beat rejection. Typically, the standard arrhythmia rejection methods interrupt data acquisition if a premature beat is detected outside of the beat length acceptance window. Rejection of the short or long beat is typical, with rejection of subsequent beat preferred. The typical beat length acceptance window for SPECT is the mean R–R′ interval ±15% to 35% but will vary depending on heart rate and rhythm. This window is generally somewhat larger than that used for planar ERNA, as significant arrhythmias may result in poor statistics, which, depending on the acquisition stop mode employed, can adversely affect the quality of the gated SPECT reconstruction. The beat length window may require widening in some patients if there is significant variation in cycle length due to either sinus arrhythmia or premature beats. Regarding acquisition stop mode, SPECT image reconstructions assume equal sampling (acquisition time) at each camera view. If several cardiac cycles are excluded due to cycle lengths falling outside the acceptance window, severe reconstruction artifacts can occur including severe streaking of the reconstructed images. For this reason, although not commonly employed, ‘‘acquisition stop for accepted beats’’ with normalization of the actual acquisition time at each projection to a common time (e.g., 30 seconds) and ‘‘acquisition stop for accepted time’’ at each projection (e.g., 30 seconds) are the preferred stop modes. Both stop for accepted beats and stop for accepted time ensure virtually identical sampling at each projection, whereas simple acquisition for camera dwell time at each projection with bad beat rejection turned on can result in some projections having no accepted beats (in the worst case) if there is a run of frequent premature beats or a drift of heart rate outside the acceptance window. As with planar studies, it is recommended that the ECG trigger point be checked to ensure that the ECG gating circuitry is gating on the upslope or peak of the ECG R-wave. The ECG gate setup should be checked with either a dual-trace oscilloscope or strip chart recorder output from the ECG gate on each patient. Since most gating devices are designed to recognize a rapid increase in QRS voltage, the optimal input to these devices is an ECG lead that is predominately a large monophasic R-wave accompanied by relatively small P-waves and T-waves and an artifact-free baseline. In most cases if the negative electrode (typically the right arm lead) is placed just below

the right clavicle in the mid-clavicular line, the positive electrode (typically the left arm lead) is placed above the costal margin 2 to 4 cm below the V4, V5, or V6 position so as to avoid overlapping the cardiac FOV, and the ground lead is placed in a similar position on the right lower chest, a good signal will be obtained. Care should be taken to carefully prepare the electrode sites with alcohol or other skin preparation materials to ensure a stable artifact-free signal. In difficult cases, a quick review of a standard 12-lead electrocardiogram may be helpful in planning electrode placement, and usually only repositioning the positive electrode will be the only required change. The ECG lead wires should be positioned so that they have no tension on them and so that neither the patient nor camera can either displace, snag, or bump them during acquisition setup and imaging, resulting in interruption of gating and/or artifacts. Bad ECG gating devices including gating devices with excessive delays between QRS onset and output of signal to the camera can adversely affect the ventricular volume curve and severely lengthen image acquisition time or result in poor statistics. ECG gating devices can be checked with commercially available dynamic phantoms.

6. *Acquisition method*. Frame mode (forward framing) is standard. However, when available, forward–backward gating should be considered, especially in patients with significant arrhythmia where the diastolic phase of the volume curve and cine displays of wall motion may be severely distorted when only forward framing is used.
7. *Frame rate*. Sixteen frames per cardiac cycle are preferred because of the poor temporal resolution of 8-frame studies. LVEF values may be decreased significantly if 8 gated frames per cycle are acquired. The statistics of SPECT acquisitions typically preclude the use of higher frame rates. An alternative to higher frame rates per cycle is to acquire 16 frames, over one half or two-thirds of the cardiac cycle, if systolic ejection parameters and EF only are required. However, with this optional acquisition mode, diastolic function analyses will be compromised if not precluded entirely.
8. *Number of projections (views) and time per view*. When using dual-head SPECT cameras, 60 or 64 projections (30 or 32 projections per head) over a 180° rotation (right anterior oblique to LPO) at approximately 30 seconds per view are preferred when (total acquisition time of about 15 or 16 minutes). Optionally, 30 or 32 views may be used (15 or 16 views per head) at 60 seconds per view for enhanced statistics in very large or severely arrhythmic patients (total acquisition time of about 15 or 16 minutes). With 3-headed systems, the total number of projections acquired over a 180° orbit and the acquisition time per projection are the same as for dual-head systems. This will require approximately 30% more total acquisition time for a 180° study. However, this 180° approach throws away half of the acquired data (i.e., in the same time required for a 180° study, a 360° study has actually been acquired). Some laboratories take advantage of all the acquired projections and reconstruct with the full 360° projection data set. This permits reduced time per projection and reduced total acquisition time with the same or greater total acquired counts for 360° reconstructions. When using a single-head gamma camera, 30 or 32 projections at 60 seconds per view are recommended (total acquisition time of about 30 to 32 minutes).
9. *Rotation*. With single- and dual-head SPECT cameras, 180° rotation is preferred; 360° rotation is optional with either a single- or dual-head camera but is not recommended unless a three-head SPECT camera is used.
10. *SPECT reconstruction/filter*. Filtered backprojection is the suggested reconstruction method. Iterative methods can also be used when available and are required if attenuation correction is performed. Different SPECT reconstruction filters are preferred by different clinical sites. The suggested filter for each of the 16 gated frames is a Butterworth filter with 0.55 Nyquist frequency cutoff, and order of 7. If the study is count-poor (due to significant arrhythmias, poor tag, or other technical reasons), a Butterworth filter with 0.45 Nyquist frequency cutoff, and order of 7 may decrease statistical noise and improve the quality of the reconstruction. As algorithms become commercially available, iterative reconstruction methods will probably become the preferred approach. Temporal filling analogous to that employed in planar imaging (I.D.2) should be applied to raw data or to transverse reconstructed images of count-poor studies.
11. *Oblique reorientation*. Preferably, each of the 16 gated frames' transverse reconstructions are reoriented in short-axis oblique slices and, optionally, long-axis coronal slices, most commonly referred to as horizontal long-axis slices, and long-axis sagittal slices, most commonly referred to as vertical long-axis slices. Typical three-dimensional (3D) reconstructions of the SPECT ERNA data are accomplished using the short-axis oblique data only. However, long-axis views are often important when observing regional wall motion by cine-loop display of the oblique reformatted slice data. See paragraph 5 in the next section.

D. Assessment of Ventricular Function—Gated SPECT ERNA Imaging: Image Display and Quantification (Table 7)

1. *LV volume curve generation*.[66-71] Most parameters describing ventricular function are extracted from a complete LV volume curve in a manner similar to that employed for planar ERNA studies. Techniques that obtain this curve from either a single two-dimensional ROI drawn at end diastole (and modified at end systole as necessary) or using multiple ROIs drawn at each time point over the summed short-axis slices, which include the entire left ventricle but exclude the left atrium, have been used on occasion in the past but are outmoded and should be avoided. Most methods described for the quantification of LV volumes from SPECT ERNA employ 3D regions encompassing the entire left ventricle, but only the left ventricle, at each frame throughout the cardiac cycle. Like methods used to quantify LV volumes from gated SPECT perfusion studies, these methods sum the calibrated voxels and partial voxels within the defined 3D LV volume throughout the cardiac cycle. Unlike planar ERNA methods that employ TACs where background subtraction is required, SPECT methods are inherently volumetric and do not typically employ background subtraction. Several automatic or semiautomatic methods have been described, which in most patients are quick and accurate, although it is important that the automatic results be checked visually and modified as necessary. Irregularities in the LV contour occasionally occur using automatic algorithms and can have significant effects on the parameters extracted from the LV curve if not manually or semiautomatically corrected during user quality assurance. Definition of the mitral and aortic valve planes is the most difficult step in this quantification—this is the result of the activities within the LV, left atrium, and aortic blood pools all being generally of similar intensity and separated only by the relatively thin and sometimes poorly defined mitral and aortic valve planes.
2. *Background*. Background subtraction is not required and generally not performed for SPECT imaging. The inherently 3D nature of reconstructed SPECT images and the 3D surface rendering of the LV blood pool employed in most quantitative methods obviate the need for background correction (see paragraph 1 above).
3. *LVEF*. As discussed in paragraph 3 above, LVEF can be computed by applying an end-diastolic ROI to end-diastolic images and an end-systolic ROI to end-systolic images reconstructed from slices summed to include the entire left ventricle (but excluding other cardiac chambers). These are essentially adaptations of gated SPECT ERNA data sets to planar ERNA quantification programs. These are outdated and to be discouraged. Automatic or semiautomatic programs which are inherently volumetric and consider the left ventricle as a 3D object are the current standard. LV

Table 7. Quantitative parameters of ventricular function-gated SPECT ERNA imaging[7,63-65]

Parameter	Method		For information, see paragraph
LV volume curve generation	Automatic ROIs at end diastole or at each time point	Preferred	1
	Manual ROI at end diastole	Standard	1
Background LVEF	None	Standard	2
	Counts-based 2D/3D method	Preferred	3
	Geometrically based method	Optional	3
	Automated method	Optional	3
	From single end diastolic ROI	Optional	3
RVEF	Not well validated at this point	Optional	4
Wall motion	3D visual assessment of movie loop	Preferred	5
	Slice-based visual assessment of movie loop	Optional	5
	Regional EF	Optional	5
LV emptying	Peak/average rate of emptying	Optional	6
LV filling	Peak/average rate of filling	Optional	7
LV volumes	Counts based	Standard	8
	Pixel based	Optional	8

volume curves can be generated and LVEFs can be computed in a manner similar to what is done with planar ERNA. Although count-based methods can be used, with SPECT, volume-based methods are preferred. Optionally, a geometric-based method may be used to compute LVEF from EDVs and ESVs. LVEFs obtained from SPECT ERNA are likely to be higher than LVEF values determined from the planar ERNA method due to the complete removal of all activity from the left atrium. Preliminary results indicate that SPECT ERNA LVEFs are approximately 7 to 10 EF units higher than those determined from planar studies.[72] Fitting the LV curve with two or three harmonics and extracting the maximum and minimum points as the EDV and ESV values are sometimes employed. Volumetric methods are generally less affected by variations in sampling at the end of the cardiac cycle due to cycle length variation. Therefore, the end-diastolic frame may occur at either the beginning or the end of the cardiac frame cycle (frame 14, 15, or 16). If a nonvolumetric activity-based method is employed and the original TAC is produced from a single end-diastolic ROI, the EFs will be consistently lower than if the TAC is produced from multiple ROIs. In this case, SPECT ERNA LVEF values may be comparable to or less than multi-ROI planar ERNA calculations. Care must be taken when applying SPECT ERNA LVEF values to the evaluation of chemotherapy patients where standards have been established using planar methods. A thorough understanding of the differences between LVEF normal values between SPECT and planar studies is required.

4. *RVEF*. Unlike planar ERNA studies, accurate computation of RVEF may be possible with SPECT ERNA due to the removal of chamber overlap and the 3D nature of SPECT. Automatic volume-based methods to date have not been as well validated as those used for the left ventricle. Some studies validating RVEF values from SPECT ERNA have yielded positive results, although others have not.[73-75] The same activity-based techniques described in paragraphs 1 and 3 above can be applied for the measurement of RVEF, but as was the case for the left ventricle, they are also discouraged for RV analysis. All of the same considerations mentioned above for the left ventricle also hold for the right ventricle, but since the RV chamber is geometrically more complex than the left ventricle, final results may vary.
5. *Wall motion*.[60,66,67,76,77] Regional wall motion in SPECT ERNA may be determined from cine displays of multiple long- and short-axis slices and from 3D displays of the cardiac chambers in cine-loop fashion (preferred). The 3D displays may be shaded-surface and/or wire-frame displays or, optionally, volume-rendered displays. These 3D images are best displayed in multiple cardinal views or rotated under user control. Cine-loop displays of long- and short-axis slices are standard on most commercial computer systems as part of gated SPECT software packages. Wall motion analyses by SPECT ERNA may be the most useful application of this technique and can be performed on most commercial systems. Optionally, regional EFs can be computed from the segmented left ventricle and have been shown to be helpful in identifying wall motion defects in patients with coronary artery disease. Alternatively, two-dimensional planar projections can be easily generated from the 3D data sets to permit viewing of cine images from a variety of projection angles.

   SPECT ERNA has been used for the assessment of left and right ventricular activation sequences and the identification of the sites of AV nodal bypass tracks, as well as LV and RV arrhythmias.[78-81] A newer application of SPECT ERNA has been the study of activation sequences to calculate parameters of ventricular synchrony such as the site of last activation useful in guiding resynchronization therapy for congestive heat failure.[82] These uses have been recently reviewed, but unfortunately, these applications currently remain available only to research laboratories since there is no commercially available software that performs these functions.[64,82]
6. *LV emptying*. LV emptying, average and maximum, may be computed in similar fashion to planar ERNA methods, as can the systolic ejection period.
7. *LV filling*. LV filling, average and maximum, may be computed in similar fashion to planar ERNA methods, as can the diastolic filling period(s).
8. *LV volumes*.[66-71] LV volumes can be accurately computed using SPECT ERNA techniques. LV surface rendering methods are inherently volumetric and are less hampered by chamber overlap. Moreover, the spatial distribution of the left ventricle is more clearly delineated. The most straightforward approach for LV volume determination that involves no geometric assumptions is to sum the 3D pixels (voxels) contained within the LV volume of interest, excluding all other structures, and multiply the number of voxels by the calibrated voxel volume. With the calibrated voxel volume (a standard system measurement on all modern SPECT systems), LV volumes at end diastole and end systole and throughout the cardiac cycle can be easily computed. Although many individual studies have compared LV volumes to those derived from cardiac contrast ventriculography going back as far as the early 1980s and, more recently, against cardiac

III. EQUILIBRIUM RADIONUCLIDE ANGIOCARDIOGRAPHY: GUIDELINE FOR INTERPRETATION (TABLE 8)

Table 8. Guideline for interpretation

		For information, see paragraph	
		Planar	**SPECT**
Display			
Quad screen cinematic display	Standard	I.D.1	II.D.1 and .5
Time smoothing	Standard	I.D.2	II.C.10
Spatial smoothing	Optional	I.D.2	II.C.10
Quality control			
Image quality			
Statistics-qualitative	Standard	I.B.2	II.C.10
Statistics-quantitative	Optional	I.C.9	II.C.8 and .10
Labeling efficiency-qualitative	Standard	I.B.2	I.B.2
Appropriate imaging angles	Standard	I.C.10	II.C.8 and .9
Appropriate zoom	Standard	I.C.2	II.C.3
Attenuation	Standard	I.F.2	-
Processing accuracy			
Ventricular ROIs	Standard	I.D.3 and .5	II.D.1 and .3
Background ROIs	Standard	I.D.4	II.D.2
Volume curve(s)	Standard	I.D.3	II.D.1
Image analysis			
Cardiac rhythm and conduction	Standard	I.D.6	II.C.5 and II.D.5
LV size			
Qualitative	Standard	I.F.4.a	II.D.8
Quantitative volume	Preferred	I.D.9	II.D.8
LV regional wall motion			
Qualitative	Standard	I.D.6	II.D.5
Semiquantitative	Optional	I.D.6	II.D.5
Quantitative	Optional	I.D.6	II.D.5
LVEF	Standard	I.D.5	II.D.3
LV diastolic filling			
Qualitative	Standard	I.D.8	II.D.7
Quantitative	Preferred	I.D.8	II.D.7
RV size			
Qualitative	Standard	I.D.11 and I.F.4.b	II.D.4
Quantitative	Optional	I.D.11 and I.F.4.b	II.D.4
RV regional wall motion	Standard	I.D.12	II.D.5
RVEF	Optional	I.D.10	II.D.4
Atrial sizes	Standard	I.F.4.c	-
Aortic and pulmonary artery sizes	Standard	I.F.7	-
LV hypertrophy	Optional	I.F.5	-
Pericardial space	Standard	I.F.6	-
Activity outside heart and great vessels	Standard	I.F.3	-
Exercise/intervention study			
Display	Standard	I.E.1	-
Regional wall motion: Changes from rest	Standard	I.E.2	-
Chamber size: Changes from rest	Standard	I.E.3	-
LVEF, RVEF: Changes from rest	Standard	I.E.4	-
Conclusion			
Correlation with clinical data	Standard	I.E.5	I.E.5
Comparison to previous studies	Standard	I.E.5	I.E.5

IV. EQUILIBRIUM RADIONUCLIDE ANGIOCARDIOGRAPHY: GUIDELINE FOR REPORTING (TABLE 9)

Table 9. Guideline for reporting

		For information, see paragraph	
		Planar	**SPECT**
Demographic data			
Name	Standard		
Gender	Standard		
Age	Standard		
Ethnic background	Optional		
Date acquisition	Standard		
Medical record number for inpatient	Standard		
Height/weight body surface area	Standard		
Acquisition parameters			
Type of study	Standard		
Radionuclide/dose	Standard		
Indication for study	Standard	I.A. and V.	I.A. and V.
Study quality	Optional	I.B.2 and I.C.6 and I.E.6	II.C.5 and .10
Results: Rest			
LV size			
Qualitative	Standard	I.F.4.a	II.D.8
Quantitative	Optional	I.D.9	II.D.8
LV regional wall motion	Standard	I.D.6	II.D.5
LV hypertrophy	Optional	I.F.5	-
LVEF	Standard	I.D.5	II.D.3
LV diastolic function			
Qualitative	Standard	I.D.8	II.D.7
Quantitative	Preferred	I.D.8	II.D.7
RV size			
Qualitative	Standard	I.D.11 and I.F.4.b	-
Quantitative	Standard	I.D.11	II.D.4
RV regional wall motion	Standard	I.D.12	II.D.5
RVEF	Optional	I.D.10	II.D.4
Atrial sizes	Optional	I.F.4.c	-
Aortic and pulmonary artery size	Optional	I.F.7	-
Results: Exercise/intervention parameters			
Type of exercise/intervention protocol	Standard	I.E.7	-
Symptom(s)	Standard	I.E.8	-
Peak heart rate and blood pressure	Standard	I.E.8	-
METS achieved or percent maximum heart rate	Optional	I.E.8	-
Results: Exercise/intervention ERNA data			
LV size: Change from rest			
Qualitative	Standard	I.E.3	II.D.5
Quantitative	Preferred	I.E.4	II.D.3
LV regional wall motion Change from rest	Standard	I.E.2	II.D.5
LVEF exercise	Standard	I.E.4	NA
RV size: Change from rest	Standard	I.E.3	-
RV regional wall motion: Change from rest	Standard	I.E.2	-
RVEF exercise	Optional	I.E.4	-

Table 9 continued

		For information, see paragraph	
		Planar	**SPECT**
Conclusion			
Normal or abnormal	Standard	I.F.8	I.F.8
Diagnostic significance of rest/exercise response	Standard	I.F.8	NA
Prognostic significance of rest/exercise response	Optional	I.F.8	NA
Comparison to previous results	Standard	I.E.5	I.E.5

NA, Not applicable; *METs*, metabolic equivalents

contrast ventriculography and gated magnetic resonance imaging (see cautions discussed in paragraph 3 above), as a caution, LV volumes have not been validated extensively with any one of the commercially available quantitative programs.[83]

V. GUIDELINES FOR CLINICAL USE OF RADIONUCLIDE ANGIOCARDIOGRAPHY

The American College of Cardiology, American Heart Association, and American Society of Nuclear Cardiology have developed guidelines for the use of radionuclide imaging of the heart. Table 10 has been adapted from these guidelines. Note that items may be categorized as class III if not enough data are presently available to substantiate routine clinical implementation.[84,85]

Table 10. Indications for equilibrium radionuclide angiocardiography (rest and/or exercise)

	Planar	**SPECT**
Diagnosis of acute coronary end diastole syndromes		
Suspected ACS in the ED with nondiagnostic electrocardiogram and biomarkers	III	III
Detection of AMI when conventional measures are nondiagnostic	III	III
Diagnosis of STE AMI	III	III
Risk assessment and assessment of prognosis and therapy after STE AMI		
Rest LV function	I	I
Rest RV function after suspected RV infarction	IIa	IIa
Presence of stress-induced ischemia and myocardium at risk	IIb	III
Detection of infarct size and residual viable myocardium	III	III
Predicting improvement in regional and global LV function after revascularization	IIb	IIb
Diagnosis, prognosis and assessment of therapy in patients with unstable angina/NSTEMI		
Measurement of LV function	I	I
Identification of ischemia in the distribution of the culprit lesion or in remote areas	IIb	III
Identification of severity and extent of disease in stabilized patients on medical therapy	IIb	III
Identification of severity/extent of disease with ongoing ischemia and nondiagnostic electrocardiogram	IIb	III
Diagnosis of myocardial ischemia when history and ECG changes are unreliable	IIb	III
Diagnosis of chronic CAD		
Assessment of ventricular performance (rest/exercise)	I/I	I/III
Diagnosis of symptomatic and selected asymptomatic patients with myocardial ischemia	IIb	III
Planning PTCA—identifying lesions causing ischemia, if not otherwise known	III	III
Risk stratification before noncardiac surgery in selected patients	IIb	III
Screening of asymptomatic patients with low likelihood of disease	III	III

Table 10 continued

	Planar	SPECT
Assessment of severity, prognosis, and risk stratification of chronic CAD		
Assessment of LV performance	I	I
Identification of extent, severity, and localization of ischemia	IIb	IIb
Risk stratification of patients with intermediate risk Duke treadmill score	III	IIb
Assessment of functional significance of intermediate coronary stenosis	IIb	IIb
Assessment of interventions in chronic CAD		
Assessment for restenosis after PCI (symptomatic)	IIb	III
Assessment of ischemia in symptomatic patients after CABG	IIb	III
Assessment 3–5 years after CABG or PCI in select patients, high-risk asymptomatic	IIb	III
Routine assessment of asymptomatic patients after PTCA or CABG	III	III
CHF		
Determination of initial LV and RV performance	I	I
RV dysplasia	IIa	IIb
Initial or serial assessment of ventricular function with exercise	IIb	III
Routine serial assessment of LV and RV function at rest	IIb	IIb
Initial and followup evaluation of LV function in patients receiving cardiotoxic drugs	I	IIb
Assessment of myocardial viability in patients with CAD and LV dysfunction	III	III
Assessment of the co-presence of coronary heart disease in patients without angina	IIb	III
Detection of myocarditis	III	III
Diagnosis and serial monitoring of hypertensive hypertrophic heart disease	IIb	IIb
Diagnosis of CAD in patients with hypertrophic cardiomyopathy	III	III
Diagnosis and serial monitoring of hypertrophic cardiomyopathy	III	III
After cardiac transplantation		
Assessment of ventricular performance	I	I
Detection and assessment of coronary vasculopathy	IIb	IIb
Valvular heart disease		
Initial and serial assessment of LV and RV function at rest	I	I
Initial and serial assessment of LV and RV function with exercise	IIb	III
Assessment of concomitant CAD	IIb	III
Congenital heart disease		
Initial and serial assessment of LV and RV function	I	I

Acknowledgement

Dr. Van Kriekinge receives partial royalties from the licensing of the Quantitative Blood Pool SPECT (QBS) algorithm owned by Cedars-Sinai Medical Center.

References

1. Recalculated dose data for 19 frequently used radiopharmaceuticals from ICRP Publication 53. Technetium-labelled erythrocytes (RBC) Tc-99m. Ann ICRP 1998;28:61.
2. Callahan RJ, Froelich JW, McKusick KA, Leppo J, Strauss HW. A modified method for the in vivo labeling of red blood cells with Tc-99m: Concise communication. J Nucl Med 1982;23:315–8.
3. UltraTag RBC. St. Louis: Mallinckrodt Medical; 1992 [package insert].
4. Gerson MC, editor. Cardiac nuclear medicine. 3rd ed. New York: McGraw-Hill, Health Professions Division; 1997.
5. Kelly MJ, Cowie AR, Antonino A, Barton H, Kalff V. An assessment of factors which influence the effectiveness of the modified in vivo technetium-99m-erythrocyte labeling technique in clinical use. J Nucl Med 1992;33:2222–5.
6. Bacharach SL, Green MV, Borer JS. Instrumentation and data processing in cardiovascular nuclear medicine: evaluation of ventricular function. Semin Nucl Med 1979;9:257–74.
7. Groch MW. Cardiac function: gated cardiac blood pool and first pass imaging. St. Louis: Mosby; 1996.
8. DePuey EG. Evaluation of cardiac function with radionuclides. In: Gottschalk A, Hoffer PB, Potchen EJ, editors. Diagnostic nuclear medicine. Baltimore: Williams and Wilkins; 1998.
9. Garcia EV. Physics and instrumentation of radionuclide imaging. Philadelphia: Saunders; 1991.
10. Garcia EV, Bateman TM, Berman DS, Maddahi J. Computer techniques for optimal radionuclide assessment of the heart. Baltimore: Williams and Wilkins; 1988.
11. Wackers FJT. Equilibrium radionuclide angiocardiography. 3rd ed. New York: McGraw Hill; 1997.
12. Bacharach SL, Green MV, Borer JS, Hyde JE, Farkas SP, Johnson GS. Left ventricular peak ejection rate, filling rate and ejection fraction: frame rate requirements at rest and exercise. J Nucl Med 1979;20:189–93.

13. Bacharach SL, Green MV, Bonow RO, Findley SL, Ostrow HG, Johnston GS. Measurement of ventricular function by ECG gating during atrial fibrillation. J Nucl Med 1981;22:226–31.
14. Strauss HW, Zaret BL, Hurley PJ, Natarajan TK, Pitt B. A scintiphotographic method for measuring left ventricular ejection fraction in man without cardiac catheterization. Am J Cardiol 1971;28:575–80.
15. Miller TR, Goldman KJ, Epstein DM, Biello DR, Sampathkumaran KS, Kumar B, et al. Improved interpretation of gated cardiac images by use of digital filters. Radiology 1984;152:795–800.
16. Steckley RA, Kronenberg MW, Born ML, Rhea TC, Bateman JE, Rollo FD, et al. Radionuclide ventriculography: Evaluation of automated and visual methods for regional wall motion analysis. Radiology 1982;142:179–85.
17. Cahill PT, Ornstein E, Ho SL. Edge detection algorithms in nuclear medicine. IEEE Trans Nucl Sci 1976;23:555–9.
18. Chang W, Henkin RE, Hale DJ, Hall D. Methods for detection of left ventricular edges. Semin Nucl Med 1980;10:39–53.
19. Jackson PC, Allen-Narker R, Davies ER, Rees JR, Wilde P, Watt I. The assessment of an edge detection algorithm in determining left ventricular ejection fraction using radio-nuclide multiple gated acquisition and contrast ventriculography. Eur J Nucl Med 1982;7:62–5.
20. Groch MW, Erwin WD, Murphy PH, Ali A, Moore W, Ford P, et al. Validation of a knowledge-based boundary detection algorithm: a multicenter study. Eur J Nucl Med 1996;23:662–8.
21. Zaret BL, Strauss HW, Hurley PJ, Natarajan TK, Pitt B. A noninvasive scintiphotographic method for detecting regional ventricular dysfunction in man. N Engl J Med 1971;284: 1165–70.
22. Pavel DG, Byron E, Bianco JA, Zimmer AM. A method for increasing the accuracy of the radionuclide measurement of ejection fraction and left ventricular volume curve [abstract]. J Nucl Med 1977;18:641.
23. Maddox DE, Holman BL, Wynne J, Idoine J, Parker JA, Uren R, et al. Ejection fraction image: A noninvasive index of regional left ventricular wall motion. Am J Cardiol 1978;41:1230–8.
24. Murphy PH. ECG gating: does it adequately monitor ventricular contraction? J Nucl Med 1980;21:399–401.
25. Cavailloles F, Bazin JP, Di Paola R. Factor analysis in gated cardiac studies. J Nucl Med 1984;25:1067–79.
26. Wendt RE, Murphy PH, Treffert JD, Groch MW, Erwin WD, Schneider PM, et al. Application and interpretation of principal component analysis of gated cardiac images [abstract]. J Nucl Med 1993;34:175P.
27. Wendt RE, Murphy PA, Schneider PM, Treffert JD, Groch MW, Ford PV, et al. Lossy compression of dynamic studies using eigenimage methods [abstract]. J Nucl Med 1994;35:P178.
28. Rosenbush SW, Ruggie N, Turner DA, Von Behren PL, Denes P, Fordham EW, et al. Sequence and timing of ventricular wall motion in patients with bundle branch block. Assessment by radionuclide cineangiography. Circulation 1982;66:1113–9.
29. Watson DD, Liedholdt EM, Carabello ME, et al. Gated blood pool imaging in patients with atrial fibrillation [abstract]. J Nucl Med 1981;22:P153.
30. Wagner RH, Halama JR, Henkin RE, Dillehay GL, Sobotka PA. Errors in the determination of left ventricular functional parameters. J Nucl Med 1989;30:1870–4.
31. Bonow RO, Bacharach SL, Green MV, Kent KM, Rosing DR, Lipson LC, et al. Impaired left ventricular diastolic filling in patients with coronary artery disease: assessment with radionuclide angiography. Circulation 1981;64:315–23.
32. Mancini GB, Slutsky RA, Norris SL, Bhargava V, Ashburn WL, Higgins CB. Radionuclide analysis of peak filling rate, filling fraction, and time to peak filling rate. Response to supine bicycle exercise in normal subjects and patients with coronary disease. Am J Cardiol 1983;51:43–51.
33. Lee FA, Fetterman R, Zaret BL, Wackers FJT. Rapid radionuclide derived systolic and diastolic cardiac function using cycle-dependent background correction and Fourier analysis. Proc Comput Cardiol 1985;443–6
34. Seals AA, Verani MS, Tadros S, Mahmarian JJ, Roberts R. Comparison of left ventricular diastolic function as determined by nuclear cardiac probe, radionuclide angiography, and contrast cineangiography. J Nucl Med 1986;27:1908–15.
35. Bauch TD, Rubal BJ, Lecce MD, Smith TE, Groch MW. S2 triggered gated blood pool imaging for assessment of diastole. Biomed Sci Instrum 1995;31:201–6.
36. Slutsky R, Karliner J, Ricci D, Kaiser R, Pfisterer M, Gordon D, et al. Left ventricular volumes by gated equilibrium radionuclide angiography: A new method. Circulation 1979;60:556–64.
37. Dehmer GJ, Firth BG, Lewis SE, Willerson JT, Hillis LD. Direct measurement of cardiac output by gated equilibrium blood pool scintigraphy: Validation of scintigraphic volume measurements by a nongeometric technique. Am J Cardiol 1981;47:1061–7.
38. Bourguignon MH, Schindledecker JG, Carey GA, Douglass KH, Burow RD, Camargo EE, et al. Quantification of left ventricular volume in gated equilibrium radioventriculography. Eur J Nucl Med 1981;6:349–53.
39. Links JM, Becker LC, Shindledecker JG, Guzman P, Burow RD, Nickoloff EL, et al. Measurement of absolute left ventricular volume from gated blood pool studies. Circulation 1982;65:82–91.
40. Massardo T, Gal RA, Grenier RP, Schmidt DH, Port SC. Left ventricular volume calculation using a count-based ratio method applied to multigated radionuclide angiography. J Nucl Med 1990;31:450–6.
41. Berger HJ, Matthay RA, Loke J, Marshall RC, Gottschalk A, Zaret BL. Assessment of cardiac performance with quantitative radionuclide angiocardiography: Right ventricular ejection fraction with reference to findings in chronic obstructive pulmonary disease. Am J Cardiol 1978;41:897–905.
42. Brent BN, Mahler D, Matthay RA, Berger HJ, Zaret BL. Noninvasive diagnosis of pulmonary arterial hypertension in chronic obstructive pulmonary disease: Right ventricular ejection fraction at rest. Am J Cardiol 1984;53:1349–53.
43. Winzelberg GG, Boucher CA, Pohost GM, McKusick KA, Bingham JB, Okada RD, et al. Right ventricular function in aortic and mitral valve disease: Relation of gated first-pass radionuclide angiography to clinical and hemodynamic findings. Chest 1981;79:520–8.
44. Maddahi J, Berman DS, Matsuoka DT, Waxman AD, Stankus KE, Forrester JS, et al. A new technique for assessing right ventricular ejection fraction using rapid multiple-gated equilibrium cardiac blood pool scintigraphy. Description, validation and findings in chronic coronary artery disease. Circulation 1979;60:581–9.
45. Pryor DB, Harrell FE, Lee KL, Rosati RA, Coleman RE, Cobb FR, et al. Prognostic indicators from radionuclide angiography in medically treated patients with coronary artery disease. Am J Cardiol 1984;53:18–22.
46. Lee KL, Pryor DB, Pieper KS, Harrell FE, Califf RM, Mark DB, et al. Prognostic value of radionuclide angiography in medically treated patients with coronary artery disease. A comparison with clinical and catheterization variables. Circulation 1990;82:1705–17.
47. Borer JS, Bacharach SL, Green MV, Kent KM, Epstein SE, Johnston GS. Real-time radionuclide cineangiography in the noninvasive evaluation of global and regional left ventricular function at rest and during exercise in patients with coronary-artery disease. N Engl J Med 1977;296:839–44.

48. Borer JS, Kent KM, Bacharach SL, Green MV, Rosing DR, Seides SF, et al. Sensitivity, specificity and predictive accuracy of radionuclide cineangiography during exercise in patients with coronary artery disease. Comparison with exercise electrocardiography. Circulation 1979;60:572–80.
49. Turner DA, Shima MA, Ruggie N, Von Behren PL, Jarosky MJ, Ali A, et al. Coronary artery disease: Detection by phase analysis of rest/exercise radionuclide angiocardiograms. Radiology 1983;148:539–45.
50. Poliner LR, Dehmer GJ, Lewis SE, Parkey RW, Blomqvist CG, Willerson JT. Left ventricular performance in normal subjects: A comparison of the responses to exercise in the upright and supine positions. Circulation 1980;62:528–34.
51. Dehmer GJ, Lewis SE, Hillis LD, Corbett J, Parkey RW, Willerson JT. Exercise-induced alterations in left ventricular volumes and the pressure-volume relationship: A sensitive indicator of left ventricular dysfunction in patients with coronary artery disease. Circulation 1981;63:1008–18.
52. Dehmer GJ, Firth BG, Nicod P, Lewis SE, Hillis LD. Alterations in left ventricular volumes and ejection fraction during atrial pacing in patients with coronary artery disease: Assessment with radionuclide ventriculography. Am Heart J 1983;106:114–24.
53. Port S, Cobb FR, Coleman RE, Jones RH. Effect of age on the response of the left ventricular ejection fraction to exercise. N Engl J Med 1980;303:1133–7.
54. Port S, McEwan P, Cobb FR, Jones RH. Influence of resting left ventricular function on the left ventricular response to exercise in patients with coronary artery disease. Circulation 1981;63:856–63.
55. Gibbons RJ, Lee KL, Cobb F, Jones RH. Ejection fraction response to exercise in patients with chest pain and normal coronary arteriograms. Circulation 1981;64:952–7.
56. Port SC, Oshima M, Ray G, McNamee P, Schmidt DH. Assessment of single vessel coronary artery disease: Results of exercise electrocardiography, thallium-201 myocardial perfusion imaging and radionuclide angiography. J Am Coll Cardiol 1985;6:75–83.
57. Wackers FJ, Berger HJ, Johnstone DE, Goldman L, Reduto LA, Langou RA, et al. Multiple gated cardiac blood pool imaging for left ventricular ejection fraction: Validation of the technique and assessment of variability. Am J Cardiol 1979;43:1159–66.
58. DePace NL, Iskandrian AS, Hakki AH, Kane SA, Segal BL. Value of left ventricular ejection fraction during exercise in predicting the extent of coronary artery disease. J Am Coll Cardiol 1983;1:1002–10.
59. Foster C, Dymond DS, Anholm JD, Pollock ML, Schmidt DH. Effect of exercise protocol on the left ventricular response to exercise. Am J Cardiol 1983;51:859–64.
60. Moore ML, Murphy PH, Burdine JA. ECG-gated emission computed tomography of the cardiac blood pool. Radiology 1980;134:233–5.
61. Corbett JR, Jansen DE, Willerson JT. Radionuclide ventriculography: I. Technical aspects. Am J Physiol Imaging 1987;2:33–43.
62. Corbett JR, Jansen DE, Willerson JT. Radionuclide ventriculography: II. Anatomic and physiologic aspects. Am J Physiol Imaging 1987;2:85–104.
63. Corbett JR. Gated blood-pool SPECT. In: DePuey EG, Berman DS, Garcia EV, editors. Cardiac SPECT imaging. New York: Raven Press; 1995. p. 257–73.
64. Ficaro EP, Corbett JR. Gated blood-pool SPECT. In: DePuey EG, Berman DS, Garcia EV, editors. Cardiac SPECT imaging. 2nd ed. Philadelphia: Lippincott Williams & Wilkins; 2001. p. 321–37.
65. Quaife RA, Corbett JR. Radionuclide ventriculography. In: McGhie AI, editor. Handbook of non-invasive cardiac testing. New York: Oxford University Press; 2001. p. 55–98.
66. Gill JB, Moore RH, Tamaki N, Miller DD, Barlai-Kovach M, Yasuda T, et al. Multigated blood-pool tomography: New method for the assessment of left ventricular function. J Nucl Med 1986;27:1916–24.
67. Corbett JR, Jansen DE, Lewis SE, Gabliani GI, Nicod P, Filipchuk NG, et al. Tomographic gated blood pool radionuclide ventriculography: Analysis of wall motion and left ventricular volumes in patients with coronary artery disease. J Am Coll Cardiol 1985;6:349–58.
68. Faber TL, Stokely EM, Templeton GH, Akers MS, Parkey RW, Corbett JR. Quantification of three-dimensional left ventricular segmental wall motion and volumes from gated tomographic radionuclide ventriculograms. J Nucl Med 1989;30:638–49.
69. Groch MW, Leidholdt EM, Marshall RA, et al. Gated blood pool SPECT imaging: Sources of artifacts [abstract]. Clin Nucl Med 1991;16:717
70. Chin BB, Bloomgarden DC, Xia W, Kim HJ, Fayad ZA, Ferrari VA, et al. Right and left ventricular volume and ejection fraction by tomographic gated blood-pool scintigraphy. J Nucl Med 1997;38:942–8.
71. Groch MW, Schippers DJ, Marshall RC, Barnett C. A quantitative program for gated blood pool SPECT imaging [abstract]. Clin Nucl Med 1991;16:713.
72. Bartlett ML, Srinivasan G, Barker WC, Kitsiou AN, Dilsizian V, Bacharach SL. Left ventricular ejection fraction: Comparison of results from planar and SPECT gated blood-pool studies. J Nucl Med 1996;37:1795–9.
73. Nichols K, Humayun N, De Bondt P, Vandenberghe S, Akinboboye OO, Bergmann SR. Model dependence of gated blood pool SPECT ventricular function measurements [see comment]. J Nucl Cardiol 2004;11:282–92.
74. Nichols K, Saouaf R, Ababneh AA, Barst RJ, Rosenbaum MS, Groch MW, et al. Validation of SPECT equilibrium radionuclide angiographic right ventricular parameters by cardiac magnetic resonance imaging [see comment]. J Nucl Cardiol 2002;9:153–60.
75. Slart RH, Poot L, Piers DA, van Veldhuisen DJ, Jager PL. Evaluation of right ventricular function by NuSMUGA software: Gated blood-pool SPECT vs. first-pass radionuclide angiography. Int J Cardiovasc Imaging 2003;19:401–7.
76. Underwood SR, Walton S, Ell PJ, Jarritt PH, Emanuel RW, Swanton RH. Gated blood-pool emission tomography: A new technique for the investigation of cardiac structure and function. Eur J Nucl Med 1985;10:332–7.
77. McGhie AL, Faber TL, Willerson JT, Corbett JR. Evaluation of left ventricular aneurysm after acute myocardial infarction using tomographic radionuclide ventriculography. Am J Cardiol 1995;75:720–4.
78. Daou D, Lebtahi R, Faraggi M, Petegnief Y, Le Guludec D. Cardiac gated equilibrium radionuclide angiography and multiharmonic Fourier phase analysis: Optimal acquisition parameters in arrhythmogenic right ventricular cardiomyopathy. J Nucl Cardiol 1999;6:429–37.
79. Botvinick EH, O'Connell JW, Kadkade PP, Glickman SL, Dae MW, Cohen TJ, et al. Potential added value of three-dimensional reconstruction and display of single photon emission computed tomographic gated blood pool images. J Nucl Cardiol 1998;5:245–55.
80. Le Guludec D, Gauthier H, Porcher R, Frank R, Daou D, Benelhadj S, et al. Prognostic value of radionuclide angiography in patients with right ventricular arrhythmias. Circulation 2001;103:1972–6.
81. Le Guludec D, Slama MS, Frank R, Faraggi M, Grimon G, Bourguignon MH, et al. Evaluation of radionuclide angiography in

diagnosis of arrhythmogenic right ventricular cardiomyopathy. J Am Coll Cardiol 1995;26:1476–83.
82. Botvinick EH. Scintigraphic blood pool and phase image analysis: the optimal tool for the evaluation of resynchronization therapy. J Nucl Cardiol 2003;10:424–8.
83. Cahill JM, Chen MY, Ficaro EP, Corbett JR, Quaife RA. Validation of 4D-MSPECT analysis method for Tc-99m gated blood pool tomography: comparison of LV ejection fractions and volumes to magnetic resonance imaging [abstract]. J Nucl Cardiol 2003;10:S20.
84. Lee TH, Udelson JE. Nuclear cardiology. In: Zipes DP, Libby P, Bonow RO, Braunwald E, editors. Braunwald's heart disease: A textbook of cardiovascular medicine. 7th ed. Philadelphia: Saunders; 2005.
85. Klocke FJ, Baird MG, Bateman TM, Berman DS, Carabello BA, Cerquerira MD, et al. ACC/AHA/ASNC guidelines for the Clinical Use of Cardiac Radionuclide Imaging. A report of the American College of Cardiology/American Heart Association Task Force on Practice Guidelines (ACC/AHA/ASNC Committee to Revise the 1995 Guidelines for the Clinical Use of Radionuclide Imaging) 2003. American College of Cardiology web site. Available from: URL: http://www.acc.org/qualityandscience/clinical/guidelines/radio/index.pdf. Accessed February 11, 2008.